Shishatskiy, S.; Pauls, J.; Pereira Nunes, S.; Peinemann, K.-V.:

Quaternary ammonium membrane materials for CO2 separation

In: Journal of Membrane Science (2009) Elsevier

DOI: 10.1016/j.memsci.2009.09.006

Quaternary ammonium membrane materials for CO_2 separation

Sergey Shishatskiy[a], Jan Roman Pauls[b], Suzana Pereira Nunes[b], Klaus-Viktor Peinemann[b]

[a] Institut für Polymerforschung
[b] Institut für Werkstoffforschung
GKSS-Forschungszentrum Geesthacht GmbH, Max-Planck-Straße 1, 21502 Geesthacht,
Germany

Abstract

Quaternary ammonium compounds are known to have extremely high affinity to carbon dioxide. Two new highly hydrophilic compounds containing one or two quaternary ammonium moieties attached to the reactive trimethoxy silane were synthesized and studied for physico-chemical and gas transport properties in the dry and wet environments. Both compounds in the form of blends with PEBAX® MH 1657 showed high CO_2 solubility coefficients and high CO_2/N_2 and CO_2/H_2 solubility selectivity. The measurements carried out with dry gases revealed the presence of specific interaction with CO_2 resulting in strong binding of the gas molecule to the polymer active center. At low temperatures CO_2 was irreversibly sorbed in the quaternary ammonium compound and was released only at temperatures higher then 60°C. For the sample modified by co-hydrolysis with TEOS the temperature of 60°C was found to be an additional transition point giving for H_2, N_2, O_2 and CO_2 break on the solubility coefficient Arrhenius plots. Measurements carried out with humid feed revealed up to 35-fold increase of gas permeability without CO_2/N_2 and CO_2/H_2 selectivity loss compared to the dry gas measurements.

Keywords

Facilitated transport, Fixed-site carrier, Quaternary ammonium, Silane, CO_2 separation, Membrane

Introduction

The reduction of the carbon dioxide waste into the atmosphere is important for the preservation of the environment at least at the current state [1]. Most of the carbon dioxide is produced when organic fuel is burned in order to produce electric energy or mechanical power [2] Electric power plants working on the fossil fuel producing enormous quantities of carbon dioxide per hour represent one of the best possibilities to reduce significantly CO_2 emission due to their steady state operating mode. Carbon dioxide can be extracted from the power plant gas streams using two methods: pre and post-combustion gas treatment.

Treatment of the post-combustion gas streams can be done by the amine treatment [3] with the consequent amine recovery. This process is expensive due to high energy consumption at the desorption stage and loss of the amine due to poisoning [4, 5].

Membrane technology can offer a competitive way of the off-gas treatment when the membrane able to work in the conditions of the power plant stack will be developed [6, 7].

The membrane should meet several requirements: High CO_2 permeance able to compensate low driving force of the separation (CO_2 content on the feed side not more then 17% [8] and no possibility to increase pressure due to enormous feed gas stream flow rate); tolerance to the trace impurities in the off-gases able to poison membrane and last but not least high water content near the dew point. [9]

The high water content in the feed gas can become beneficial for the gas separation process when one consider the choice of the membrane's selective layer material. The material has to be in the rubber state since carbon dioxide permeance should significantly exceed the one of nitrogen. The best solution would be the material with the diffusion selectivity as close to 1 as possible and with the solubility selectivity CO_2/N_2 as high as possible. The lowest diffusion selectivity can be achieved in the liquid membranes and the highest solubility selectivity in the materials specifically interacting with CO_2.

CO_2 is quite soluble in many polymers, what can be used as an advantage for developing membranes with preferential CO_2 transport. The gas solubility in polymers increases with increasing condensability [10], but also is highly influenced by specific interactions. Polyfluoroacrylates and polyfluorophosphazines are known for the very high CO_2 solubility [11, 12]. Poly (dimethylsiloxane) (PDMS) has the highest solubility among the non-fluorinated polymers, due to low cohesive energy allied to low glass transition and high flexibility, as well as some contribution of Lewis acid-Lewis base interaction. However PDMS is highly permeable for most gases and the CO_2 selectivities are too low to lead to effective membranes. Oxygenated polymers are characterized by a strong Lewis acid-Lewis base interaction interaction between the C atom of CO_2 and the lone electron pairs on oxygen (e. g. in carbonyl groups), as well as between the oxygen atoms of CO_2 and the hydrogen atoms attached to the carbonyl carbon. Polymers and copolymers containing ethylene oxide segments have been intensively investigated for CO_2 permeation with a very good balance of high selectivity and permeability [13-17]

The solubility of CO_2 in polymers can be much stronger influenced if specific “reactive sites” are present, which enable facilitated transport by reversible reaction between gas and polymer [18]. Good examples of “reactive groups” for CO_2 are primary and secondary amines, with electron donating nitrogen, acting as Lewis bases in contact with CO_2. The following reversible reactions are then possible:

$$\text{Primary amine: } 2\ RNH_2 + CO_2 \leftrightarrow RNHCO_2^- \text{ (carbamate)} + RNH_3^+$$

$$\text{Secondary amine: } 2\ R_2NH + CO_2 \leftrightarrow R2NCO_2^- \text{ (carbamate)} + R_2NH_2^+$$

Exceptionally high CO_2/N_2 selectivity values have been reported for polyvinylamine [19]. Polyethyleneimine has been investigated for facilitated transport membranes for CO2 for many years [20, 21].

Tertiary amines do not react with CO_2 forming carbamate at least in the dry state. Only in the presence of water a reversible reaction is possible, making the performance of membranes with ternary amine sites much more dependent on the environment humidity:

$$\text{Tertiary amine: } R_3N + H_2O + CO_2 \leftrightarrow R_3NH^+ + HCO_3^-$$

However interactive sites like tertiary amine not always stimulate the CO_2 solubility in polymers. The self interaction between amine groups might be stronger than the CO_2 –moiety interaction [12].

Hydroxy groups react forming bicarbonate ions:

$$OH^- + CO_2 \leftrightarrow HCO_3^-$$

In this way poly (vinyl alcohol) is reported as selective membrane material for CO_2 [22]. The alcohol groups can also contribute to solubility by hydrogen bonding. Chitosan has a primary amine and two hydroxyl groups, being also under investigation for CO_2 membrane development [23].

Ionic liquids and polymers with quaternary ammonium groups have also been reported with high CO_2 solubility [24] and high selectivity for CO_2/N_2 or CO_2/H_2 [25-27]

In the case of polyelectrolyte with quaternary nitrogen groups the reaction with CO_2 is claimed to involve the hydrated counter-ion, rather than the pending cationic group [18], like described here:

$$2\ X^-.4\ H_2O + CO_2 \leftrightarrow HCO_3^- + HX_2^-.\ 7H_2O$$

However changes in the structure of the “polymerized ionic liquid”, e. g. by introducing ether segments, might improve considerably the performance [25]. The membrane performance is highly dependent on the environmental humidity level.

The aim of the current work is the development of new CO_2 selective organic-inorganic materials with active sites for CO_2 sorption leading to high solubility selectivity. The membrane material should be able to swell at the conditions of the feed gas stream thus providing the diffusivity selectivity close to unity. The mechanical stability and the degree of swell of the selective materials can be controlled by the content of inorganic segments and crosslinks. Furthermore the membrane production is aimed to be performed with environmentally friendly solvents like light alcohols and water.

Experimental

Materials

(3-Aminopropyl)triethoxysilane (APTES), glycidyltrimethylammonium chloride (ClycAmCl) (solution containing 20 wt.% water), tetraethoxysilane (TEOS), ethanol, methanol, hydrochloric acid, acetic acid and ammoniac solution were purchased from Sigma-Aldrich and used as received. High purity deionized water having conductivity 0.06µS cm^{-1} was used for hydrolysis and membrane preparation. PEBAX® MH 1657 (Arkema) (containing 60 wt.% of PEO and 40 wt.% PA-6) was used as received for membrane preparation.

Characterization methods

Thermal analysis was carried out by using a Netsch DSC 204 differential scanning calorimeter and a Netsch TG 209 thermogravimetric analyzer.

The pH of the solutions was determined and titration was carried out using Inolab 730 pH meter.

The diffusion, permeability and solubility of pure H_2, He, N_2, O_2 and CO_2 in dry membrane samples were measured at feed pressures 0.3-1.7 bar and temperatures 10 – 120°C using a constant volume / variable pressure experimental setup described elsewhere [14, 28]. All measurements were repeated at least 3 times and the result was considered as acceptable when the values of permeability and diffusion coefficient had scattering less then 5%. The evacuation time for the membrane degassing was chosen taking in account the results of each experiment, being not shorter then 6 time-lags for all gases except CO_2 when the evacuation time was increased to 8 time-lags.

The permeability coefficient was calculated according to the formula:

$$P = D \cdot S = \frac{V_p \cdot l}{A \cdot R \cdot T \cdot \Delta t} \ln\left(\frac{p_f - p_{p1}}{p_f - p_{p2}}\right) \qquad (1)$$

where D is the diffusion coefficient and S in the sorption (solubility) coefficient of the gas under study, V_p is the permeate volume; l – the membrane thickness; A – the membrane area; R – the gas constant; Δt – the time difference between two points (1 and 2) on the pressure increase curve; p_f – the feed pressure considered constant in the time range Δt and p_{p1} and p_{p2} are permeate pressures at time moments 1 and 2.

The diffusion coefficient was calculated using formula:

$$D = \frac{l^2}{6\theta} \tag{2}$$

where θ is the time-lag.

Activation energies of all gas transport parameters were determined from the Arrhenius plots of the temperature dependences of permeability diffusion and solubility coefficients according to the formulas:

$$P = P_0 \exp\left(\frac{-E_P}{RT}\right)$$

$$D = D_0 \exp\left(\frac{-E_D}{RT}\right) \tag{3}$$

$$S = S_0 \exp\left(\frac{-\Delta H_S}{RT}\right)$$

Where P_0, D_0 and S_0 are pre-exponential constants, E_p, E_d are permeation and diffusion activation energies and ΔH_s is the change in enthalpy of sorption. The last three parameters are related according to the solution-diffusion model [29]:

$$E_p = E_D + \Delta H_S \tag{4}$$

The transport parameters of the same membranes in wet environment were determined on the constant volume / variable pressure experimental setup, where feed gas stream was humidified to the water partial pressure close to the dew point. Due to experimental setup limitations experiments were carried out at atmospheric pressure at 23 and 60 °C.

In the presence of the water vapor in the feed gas stream changes the experimental steps and conditions have to be different than those followed in the dry gas “time-lag” measurement. Single gas measurements are carried out with the polymeric membrane completely free of any volatile impurities, like typically obtained by routine preparation and after final degassing in the experimental setup. On the other hand, humid gas measurements are considered as experiments with gas mixtures. In this case diffusion and solubility data can not be obtained, since the membrane at the beginning of the experiments is already exposed to the “gas mixture” and can be only characterized at the steady state gas flow. For measurement in the presence of water vapor the membrane is exposed to the humid gas as long as necessary to establish a final gradient of water concentration considered close to the equilibrium state.

The treatment of the wet gas experimental results is not obvious [30]. In this case two gases penetrate the membrane simultaneously and the pressure on the permeate side is registered with only one and non-selective pressure sensor. Fortunately water permeates through any polymer with a rate several orders of magnitude faster then any other permanent gas (Figure 1). The water pressure on the permeate side equilibrates with that on the feed side very fast and any further permeate pressure increase can then be attributed only to the permeation of the gas under investigation, which is much slower. The permeability coefficient for a certain gas through a membrane of known thickness can be calculated, by taking the slope of the final part of the permeate pressure increase curve.

Membrane preparation

Membranes of polysilsesquioxanes with quaternary ammonium groups.

Trimethoxysilanes were synthesized with one ($1N^+$) or two ($2N^+$) ammonium chloride groups (structure depicted in Scheme 1) by the reaction of APTES and GlycAmCl mixed at the corresponding molar ratios. The reaction was conducted by mixing of the two aforementioned immiscible liquids in a round bottom flask and stirring it over night at 60°C. After 12 hours mixing the previously turbid white emulsion became a transparent and colorless very viscous liquid with a minor amine odor.

The obtained ammonium modified silane was then diluted with methanol and stirred for more 24 hours at the reflux conditions (about 65 °C). Ethanol was not used as solvent to avoid any eventual effect of shifting the hydrolysis of the silane. The GlycAmCl contained up to 20% water when purchased and added to the reaction mixture. This water might start the hydrolysis of the silane even at the first reaction steps, forming the structure depicted in Scheme 2 for the $2N^+$ compound.

After the synthesis the remaining solvent was evaporated in a rotavapor at 80°C with vacuum of ca. 10 mbar and further dried in the vacuum oven at 100°C for 12 hours. Upon drying the both obtained compounds were colorless transparent rigid solids with a minor amine odor.

Membranes were prepared by casting the solution of hydrolyzed silanes on glass plates coated with Teflon.

Membranes of polysilsesquioxanes blended with PEBAX® MH 1657

Membranes were prepared from solutions in water/ethanol 30/70 wt % mixture. 3wt % PEBAX solution was previously prepared by dissolving polymer pellets in the water/ethanol mixture and stirring in a closed glass bottle at 80°C. Then a solution of the xN^+ compound (usually 10 wt % in water/ethanol) was added. The final solution was stirred for at least one hour and then poured into a leveled Teflon Petri dish. The solvent mixture was allowed to evaporate at 35°C and the obtained membrane was removed from the Petri dish and dried in the vacuum oven at 100°C for 24 hours.

Before the measurement the membrane was additionally dried in a high vacuum oven at 100°C for at least 12 hours then transported between two hot glass plates to the experimental setup, cut and placed into the measurement cell. In order to reduce the air exposure time and eventual uncontrolled water absorption, the thickness of the membrane was determined only after all gas transport measurements were done and the membrane was removed from the cell. All the obtained blend membranes were homogeneous and even more transparent then pure PEBAX membranes.

Membranes of polysilsesquioxanes with quaternary ammonium groups prepared with TEOS

In order to increase the molecular weight of the $1N^+$ and $2N^+$ compounds hydrolysis reactions in the presence of TEOS as co-monomer were carried out. The quaternary ammonium compound was dissolved in methanol, titrated with 0.01M solution of hydrochloric acid in methanol to the $pH<7$. Then 18 mol % TEOS (to xN^+ compound) was added to the solution and stirring started. The necessary water for the hydrolysis was added in 3-fold excess to stoichometry, taking into account the water provided by concentrated HCl. The structure of the possible $2N^+$ polymer obtained after the hydrolysis is presented in Scheme 3.

Results and discussion

The membranes prepared in this work have hydroxyl, quaternary ammonium and amine groups, which are available for facilitated transport of CO_2 in the presence of water.

Both $1N^+$ and $2N^+$ synthesized compounds are extremely hydrophilic, able to absorb water from the atmosphere. The compounds are soluble in water and methanol, have limited solubility in ethanol and are not soluble in any of other organic solvents (THF, γBL, NMP, cyclohexane).

Thermal gravimetric analysis showed (Figure 2) that after drying in vacuum both compounds contain minor, not more then 3 wt%, quantities of volatile solvent and are stable up to at least 200 °C. The difference of the residue at 600°C corresponds to the chemical structure of the quaternary ammonium compounds and is consistent with the silica content in $1N^+$ and $2N^+$ (Table 1).

The DSC curves (Figure 3) showed well resolved glass transitions at 22°C for both compounds, which might be related to the inorganic segments resulted from hydrolysed silanes. The curves for both compounds show no evidence of crystallinity. The transition at 0°C is due to solved or even coordinated water, confirming that this water can be hardly removed from the membrane, even after heating the sample up to 120°C.

At 49 and 65°C, respectively for $1N^+$ and $2N^+$, another transition can be observed, which might be related to the quaternary ammonium and/or amine groups.

Aqueous solutions of the $1N^+$ and $2N^+$ compounds have a basic nature caused by the residual secondary and tertiary amines. Titration of the aqueous solutions was carried out using 1M hydrochloric acid aqueous solution (Figure 4). In order to determine the reproducibility of the results a number of solutions was freshly prepared using $1N^+$ taken from different synthesis batches. It was found that the pH drop point deviation is minimal and is around 1.2 molecules of HCl to 1 molecule of $1N^+$ (blue line). When the solution is exposed to the air for a long time (4 months) it absorbs CO_2 and the number active of centers available for HCl is reduced causing lower basicity (red line). $2N^+$ compounds have stronger basic sites than $1N^+$ and are able to coordinate 1.45 molecules of HCl per molecule.

Permeability, diffusion and solubility coefficients were determined for the dry blend membranes of $1N^+$ or $2N^+$ compounds and PEBAX MH 1657. The samples prepared by hydrolysis of the compounds depicted in Scheme 1 formed films but were too brittle in the completely dry state to be cut and fixed in measurement cells. The products analogous to that depicted in Scheme 2 did not have high molecular weights due to the steric hindrances for further polymerization, causeds by the quaternary ammonium groups. Additionally excessive water absorption from the atmosphere leads to lack of dimensional stability. These problems could be minimized by blending the hydrolyzed silanes with PEBAX MH 1657 before preparing the membranes.

PEBAX MH 1657 was found to be compatible with the synthesized compounds in a wide range of concentrations. PEBAX /xN^+ blend membranes were mechanically stable when the xN^+ compound content was up to 60 wt%. Blends of 50 wt% PEBAX and 50 wt % of quaternary ammonium compounds could then be tested, measuring diffusion, permeability and the most important parameter the CO_2 solubility coefficients.

The DSC analysis of the blends revealed a melting peak with a maximum at 20 °C, which is characteristic for the ethylene oxide block of PEBAX. By blending with PEBAX the water uptake was 35 wt % reduced and the mechanical integrity was considerably increased.

Measurements of H_2, O_2, N_2 and CH_4 permeation through 2N^+/PEBAX membranes were performed (three repeating measurements per gas) in a constant volume/variable pressure equipment. For all the 4 gases a standard behavior expected for inert gases was observed. However the carbon dioxide measurements had a completely different pattern. It was found that at temperatures bellow 60°C the evacuation time of 8 time-lags was not enough to release the CO_2 molecules bonded to the active centers (amine and ammonium sites) of the xN^+ compound (Figure 5).

It is interesting to see that by taking the longest time-lag obtained at each temperature a perfect Arrhenius plot could be obtained (Figure 6). The difficulty with CO_2 desorption bellow 60°C was minimized with the introduction of additional 90°C heating/cooling cycles before each experiment. Since the presence of non-desorbed CO_2 could in fact alter the membranes properties and influence the measurements of other gases, the measurement routine was changed: at first H_2, O_2 and N_2 were tested at different temperatures and only then CO_2 was used.

The gas transport properties of 1N^+/PEBAX membrane were measured in dry (Table 2) and humid conditions. The experiments (dry and humid) were performed at 23 and 28°C. Higher temperatures were also adopted for the dry characterization. Experiments in the presence of water were carried out at 60°C as well, but when the CO_2 was transported through the membrane it swelled excessively and lost the integrity. This was an indication that additional crosslinking was necessary and this was carried out later.

The permeation of all gases through the $1N^+$/PEBAX membrane (Table 2) in the dry state is slower than that observed through pure PEBAX membrane (Table 3). The CO_2 solubility in the $1N^+$/PEBAX membrane was nearly 15-fold higher than in PEBAX, while the N_2 solubility did not increase more than 1.5-fold with the incorporation of the quaternary ammonium hydrolyzed silane.

It was expected that in the presence of water the membrane would swell enough to bring the diffusion selectivity close to unity, leading to much higher permeability selectivity for CO_2 over other gases. However when the membrane was tested in the humid environment at 23°C the permeability of both CO_2 and N_2 has increased significantly but, unfortunately, to the same degree and the resulting selectivity did not increase as expected:

$$P(CO_2) = 600 \text{ Barrer};\ P(N_2) = 10 \text{ Barrer};\ \alpha(CO_2/N_2) = 60$$

The CO_2/N_2 selectivity increased from 53 to 60. Nearly 35-fold increase of the permeability coefficients indicates a significant swelling of the $1N^+$/PEBAX membrane in the presence of water. Analogous measurements done with pure PEBAX membrane show that the CO_2 permeability just increases less than twice in the presence of water:

$$P(CO_2) = 160 \text{ Barrer};\ P(N_2) = 3.3 \text{ Barrer};\ \alpha(CO_2/N_2) = 48.5$$

In contrast to $1N^+$/PEBAX membranes the selectivity α (CO_2/N_2) for pure PEBAX dropped. For pure PEBAX no specific facilitated transport of CO_2 occurs. On the other hand the counterions of the quaternary ammonium sites in the $1N^+$/PEBAX membrane are expected to strongly interact with CO_2 in the presence of water, increasing considerably the preferential transport.

$2N^+$/PEBAX blends in the dry state have lower CO_2/N_2 selectivity, although the solubility selectivity was higher than those containing $1N^+$. The system has two times more quaternary ammonium groups, but it does not have secondary amines, which might support the CO_2 facilitated transport even in the absence of water. Tertiary amines as well as the counter-ions of the quaternary ammonium groups can only contribute for CO_2 facilitated transport in the presence of water.

Measurements with humid gases led to the following results:

$$P(CO_2) = 440 \text{ Barrer};\ P(N_2) = 9{,}0 \text{ Barrer};\ \alpha(CO_2/N_2) = 49$$

The CO_2/N_2 selectivity for $2N^+$/PEBAX blends increased from 38 to 49, confirming that it is more sensitive to the presence of water than in the case of $1N^+$/PEBAX.

Figure 7 and 8 show the dependence of the time-lag, diffusion coefficient, permeability and solubility on the feed pressure. The values are practically constant for the inert gases, as shown for N_2 in Figure 7. On the other hand for CO_2 (Figure 8), while permeability stayed practically constant, the dependences of solubility, diffusion coefficient and time-lag on pressure are evident. This might be related to the facilitated transport mechanism associated to the CO_2 permeation in these membranes, although for other facilitated transport membranes previously reported in the literature a dependence of permeability on pressure is also observed. As mentioned in the introduction the interaction between CO_2 and the $2N^+$ compounds requires some water to activate the facilitated transport. This is valid for tertiary amines and the counter-ions of the quaternary ammonium groups. Taking in account Figure 3 it seems that some water is kept in the membrane even after long drying periods under vacuum and heating. El Azzami and Grulke [23] discussed the role of water in the CO_2 through chitosan membranes and their consideration can be also used here. Two kinds of water are possible in the polymer matrix: free water, which can be easily lost above 110°C, and bonded water (bonded for instance through hydrogen bonds). The bonded water can only be lost above 140°C. Both types of water seem to facilitate the complexing of carbon dioxide with the polymer.

Additionally OH groups might also contribute for acid-base interaction with CO_2. By increasing the pressure the sites for interaction become partially saturated and solubility decreases. Once the reactive sites are not available anymore, the CO_2 molecules can move more freely with a consequent reduction of time-lag and increase of diffusion coefficient. Since in the case of these compounds the changes in solubility and diffusivity compensate each other, the permeability is kept constant with pressure.

Membranes with TEOS

Membranes were prepared analogously to those based on $2N^+$/PEBAX blends, as described before. However TEOS was used as co-monomer to increase the degree of crosslinking and the molecular weight of the $2N^+$ compound. The resulting titrated and hydrolyzed ($2N^+$TEOS) compound was colorless, brittle and highly hydrophilic solid. The $2N^+$TEOS compound was still soluble in water, methanol and water/ethanol mixture. Unfortunately also with the addition of TEOS the material was brittle and did not lead to membranes with good mechanical properties. All gas transport experiments were performed as before with membranes prepared from blends with 50% PEBAX. The membranes prepared with addition of TEOS, in opposite of those prepared before were partially turbid, indicating phase separation. This can be attributed to the increased molecular weight of the $2N^+$TEOS compound and particularly to the increase of content of inorganic segments in the polymer, with consequent decrease of compatibility with PEBAX.

The gas transport properties of the $2N^+$TEOS/PEBAX membrane were investigated in the temperature range 20-90°C. The first set of experiments was carried out without CO_2 measurements; increasing the temperature; the second set was carried out with temperature decrease for all 4 gases under study. The solubility values for H_2, N_2 and O_2 practically remained the same. The solubility of CO_2 in the membrane decreased practically 20-fold, since with the introduction of more inorganic non-functionalized segments a number of “reactive sites” is lost. The diffusion coefficient of all inert gases decreased, since more rigid inorganic segments were included, but the diffusion coefficient of CO_2 increased at the measuring temperature of 28^{o}C, indicating that the CO_2 molecules move with more freedom, since there are less “reactive sites” to interact.

Very low solubility activation energy was observed for inert gases (Table 5). The simultaneous increase of the diffusion and permeability coefficients with temperature give nearly zero slopes for the solubility coefficient dependences on temperature causing in some cases positive ΔH_S values. This behavior is not unknown for polymers. Sorption enthalpies as low as -2±2 kJ/mol were reported for polymers with ethylene oxide segments [31], which corresponds to the range of experimental error of values obtained in the current work. The absence of a high slope in the solubility coefficients temperature dependence made it easier to observe steps in curves for O_2 and N_2 (Figure 9) near about 60°C. For the other membranes analogous behavior might have been masked by the experimental data scattering. Also for the hydrogen diffusivity coefficient curve as a function of temperature (Figure 10) a discontinuity can be seen around the same temperature. This observation can be correlated to thermal transitions or rearrangements of the polymer matrix. In Figure 3, the DSC of $2N^+$ compounds shows a transition around 65^{o}C. The transition might be related to weakening of self interaction of the tertiary amine group bonded to which the quaternary ammonium groups are attached. This might lead to more flexibility in the polymer matrix. Kim et al. [32] reported discontinuity of permeability curves as a function of temperature for PEBAX and related this also to transitions related to the polyamide block of PEBAX, observed by DSC. A similar contribution might also additionally come from the

PEBAX constituting the $2N^+TEOS$/PEBAX membrane. For other blends also with PEBAX the effect was barely observed (e. g. Figure 6).

Also around 60°C, a change in slope of the CO_2 diffusivity coefficient (D) and permeability (P) curves as a function of temperature (Ahrrenius plot, Figure 11) can be clearly seen. As a consequence two activation energies can be calculated above and below the transition temperatures, both for D and P. They are listed in Table 6. Above 60 °C the activation energies for diffusion and permeation are lower than below this temperature. A similar observation was reported for chitosan membranes, which contain amine groups for CO_2 facilitated transport [23]. For the lower temperature range the Ahrrenius plot reflects the facilitated transport process, which is then the dominating mechanism. In the higher temperature range, the contribution of the facilitated transport mechanism decreases. Facilitated transport of molecules like oxygen in a complexing membrane has been classically explained making use of a dual-mode sorption model [33, 34]. Rapid and reversible sorption and desorption of specific gas molecules by strong interaction with complexing sites follow a Langmuir isotherm, while the non-specific interaction gas-polymer follows the Henry's Law. The contribution of the Langmuir mode is expected to be larger at low pressure and low temperature conditions and the Henry's law mode. An increase of both diffusion coefficients for the Henry (D_H) and the Langmuir-type diffusion (D_L) can be usually attributed to a usual increase of free volume of polymers with increase of temperature. An increase of the D_H/D_L ratio with increasing temperature corresponds to an increase of the dissociation rate constant of the reversible bond between gas molecule and complexing site in the polymer.

Conclusions

The process of the carbon dioxide sequestration from the off-gases of the fossil powered power plant requires a membrane with high permeance as well as high CO_2/N_2 selectivity. The presence of high water vapor content in the off-gas leads to the possibility of developing a membrane able to swell in the feed gas stream and separate gases not by the diffusion but solubility selectivity.

Two compounds having one or two quaternary ammonium moieties were synthesized and polymerized via hydrolysis of the triethoxysilane moiety. Both synthesized compounds are thermally stable up to 200°C, have glass transition at 22°C are soluble in water and low alcohols.

Despite the presence of the silane groups aqueous solutions of both compounds having pH=10.5 were stable in time. The titration of initially basic solutions with 0.01M HCl showed that $1N^+$ and $2N^+$ compounds could coordinate up to 1.2 and 1.4 molecules of HCl respectively.

Gas transport properties of the xN+/PEBAX blend membranes were measured in dry and wet environment.

Dry gas measurement allowed determining the dependence of permeability, diffusion and solubility coefficients on temperature and feed pressure. It was found that CO_2 is irreversibly sorbed on the active centers of the quaternary ammonium compounds at temperatures lower then 60°C and can be released only with heating above this temperature. At the same temperature the Arrhenius plots of gas transport parameters for $2N^+$ compound hydrolyzed in the presence of TEOS showed stepwise deviation from linearity, the property similar to the glass transition.

High affinity to CO_2 was found for both compounds leading to the CO_2/N_2 solubility selectivity up to 1500. Humid gas measurements showed strong increase of the permeability coefficients for all gases without the selectivity loss compared to the dry gas measurements. CO_2 permeability up to 600 Barrer was measured in humid environment.

Both synthesized compounds and their copolymers with TEOS showed promising gas separation properties prosperous for the development of the composite membrane for CO_2 separation in humid environments.

Acknowledgements

Authors are grateful to Michael Schossig for his input into the design of the humid gas permeation experimental setup and measurement routine. The work was supported by the Helmholtz-Alliance MemBrain (Gas Separation Membranes for Zero-Emission Fossil Power Plants).

References

[1] Kyoto Protocol to the United Nations Framework Convention on Climate Change, United Nations, 1998, http://unfccc.int/essential_background/kyoto_protocol/items/678.php

[2] Emissions of Greenhouse Gases in the United States 2007, U.S. Department of Energy, 2008

[3] P.M.M. Blauwhoff, G.F.Versteeg, W.P.M. van Swaaij, A study on the reaction between CO_2 and alkanolamines in aqueous solutions, Chem. Eng. Sci. 39 (1984) 207-225

[4] A.B. Rao, E.S. Rubin, A technical, economic and environmental assessment of amine-based CO2 capture technology for power plant green gas control, Environmental Science and Technology, 36 (2002) 4467-4475

[5] H. Undrum, O. Bolland, E. Aarebrot, Economic assessment of natural gas fired combined cycle power plant with CO2 capture and sequestration, Proceedings of the 5th Greenhouse Gas Control Technologies Conference (GHGT5), 13-16 August 2000,, Cairns, Australia, CSIRO Publishing

[6] S. P. Kaldis, G. Skodras, G. P. Sakellaropoulos, Energy and capital cost analysis of CO_2 capture in coal IGCC processes via gas separation membranes, Fuel Processing Technology, 85 (2004) 337-346

[7] L. Zhao, E. Riensche, R. Menzer, L. Blum, D. Stolten, A parametric study of CO2/N2 gas separation membrane processes for post-combustion capture, J. Membr. Sci., 325 (2008) 284-294

[8] K. Thambimuthu, J. Davison, M. Gupta, CO_2 capture and reuse, in: Proceedings of the IPCC Workshop on Carbon Dioxide and Storage, Regina, Canada, November 18–21, 2002

[9] L. Deng, T.-J. Kim, M.-B. Hägg, Facilitated Transport of CO_2 in novel PVAm/PVA blend membrane, J. Membr. Sci., (2008), in press, doi:10.1016/ j.memsci.2009.05.019

[10] H. Lin and B. Freeman, Materials selection guidelines for membranes that remove CO2 from gas mixtures, J. Molecular Structure 739 (2005) 57-74

[11] M. L. O'Neill, Q. Cao, M. Fang, and K. P. Johnston, S. P. Wilkinson and C. D. Smith, J. L. Kerschner and S. H. Jureller, Solubility of Homopolymers and Copolymers in Carbon Dioxide, Ind. Eng. Chem. Res. 37 (1998) 3067-3079

[12] S. Kilic, Y. Wang, J. K. Johnson, E. J. Beckman, R. M. Enick, Influence of tert-amine groups on the solubility of polymers in CO_2, Polymer, 50 (2009) 2436-2444

[13] I. Blume, I. Pinnau, Composite membrane, method of preparation and use ,US Patent 4963165

[14] A. Car, C. Stropnik, W. Yave, K. V. Peinemann, PEG modified poly(amide-b-ethylene oxide) membranes for CO_2 separation, J. Membr. Sci., 307 (2008) 88-95

[15] A. Car, C. Stropnik, W. Yave, K. V. Peinemann, Pebax$^{®}$/polyethylene glycol blend thin film composite membranes for CO_2 separation: Performance with mixed gases, Sep. Pur. Tech., 62 (2008) 110-117

[16] M. L. Sforça, I. V. Yoshida, S. P. Nunes, Organic–inorganic membranes prepared from polyether diamine and epoxy silane, J. Membr. Sci., 159 (1999) 197-207

[17] H. Lin, E. Van Wagner, B. D. Freeman, L. G. Toy, R. P. Gupta, Plasticization-Enhanced Hydrogen Purification Using Polymeric Membranes, Science, 311 (2006) 639-642

[18] M. B. Hägg, R. Quinn, Polymeric Facilitated Transport Membranes for Hydrogen Purification, MRS Bulletin, 31 (2006) 750-755

[19] M. B. Hägg, A. Lindbrathen, CO_2 Capture from natural gas fired power plants by using membrane technology, Ind. Eng. Chem. Res. 44 (2005) 7668-7675

[20] J.G. Tajar, I.F.Miller, Permeation of carbon dioxide, oxygen and nitrogen through weakly basic polymer membranes, AIChE J., 18 (1972) 78–83

[21] H. Matsuyama, A. Terada, T. Nakagawara,Y. Kitamura, M. Teramoto, Facilitated transport of CO2 through polyethylenimine/poly(vinyl alcohol) blend membrane, J. Membr. Sci. 163 (1999) 221–227

[22] J. Zou, W. S. Ho, CO_2-selective polymeric membranes containing amines in crosslinked poly(vinyl alcohol), J. Membr. Sci., 286 (2006) 231-310

[23] L. A. El-Azzami, E. A. Grulke, Carbon dioxide separation from hydrogen and nitrogen facilitated transport in arginine salt-chitosan membranes, J. Membr. Sci. 328 (2009) 15-22

[24] A. Blasig, J. Tang, X. Hu, S. P. Tan, Y. Shen, M. Radosz, Carbon Dioxide Solubility in Polymerized Ionic Liquids Containing Ammonium and Imidazolium Cations from Magnetic Suspension Balance: P[VBTMA][BF_4] and P[VBMI][BF_4], Ind. Eng. Chem. Res., 46 (2007) 5542-5547

[25] J. E. Bara, C. J. Gabriel, E. S. Hatakeyamaa, T. K. Carlisle, S.Lessmann, R. D. Noble, D. L. Gin, Improving CO_2 selectivity in polymerized room-temperature ionic liquid gas separation membranes through incorporation of polar substituents, J. Membr. Sci., 321 (2008) 3–7

[26] R. Quin, D. V. Laciak, Polyelectrolyte membranes for acid gas separations, J. Membr. Sci., 131 (1997) 49-60

[27] R. Quinn, A repair technique for acid gas selective polyelectrolyte membranes, J. Membr. Sci,. 139 (1998) 97-102

[28] S. M. Shishatskiy, Yu. P. Yampolskii, K. V. Peinemann, Effects of film thickness on density and gas permeation parameters of glassy polymers, J. Membr. Sci., 112 (1996) 275-285

[29] J.G. Wijmans, R. W. Baker, The Solution-Diffusion Model: A Unified Approach to Membrane Permeation, in Yu. Yampolskii, I. Pinnau, B. Freeman (Eds), Materials Science of Membranes for Gas and Vapor Separation, Wiley 2006

[30] S. J. Metz, Water vapor and gas transport through polymeric membranes, PhD Thesis, Twente University, 2003.

[31] H. Lin, E. Van Wagner, J. S. Swinnea, B. D. Freeman, S. J. Pas, A. J. Hill, S. Kalakkunnath, D. S. Kalika, Transport and structural characteristics of crosslinked poly(ethylene oxide) rubbers, J. Membr. Sci., 276 (2006) 145-161

[32] J. H. Kim, S. Y. Ha, Y. M. Lee, Gas permeation of poly(amide-6-b-ethylene oxide) copolymer, J. Membr. Sci., 190 (2001) 179–193

[33] H. Nishide, M. Ohyanagi, Y. Funada, T. Ikeda, E. Tsuchida, Oxygen Transport Behavior through the Membrane Containing a Fixed Carrier and Adhered to a Second Polymer, Macromolecules, 20 (1987) 2312-2313

[34] H. Nishide, M. Ohyanagi, K. Suenaga, E. Tsuchida, J. Polymer Sci. Part A: Polymer Chemistry, 27 (1989) 1439-1443

List of Tables, Schemes and Figures

Tables

Table 1. Comparison of the experimental (TGA) and calculated residue values for $1N^+$ and $2N^+$ compounds

Table 2. Gas transport properties of the $1N^+$/PEBAX blend membrane measured in the dry state at 23°C.

Table 3. Gas transport parameters of pure dry PEBAX MH 1657membrane measured at 28°C

Table 4. Gas transport properties of the $2N^+$/PEBAX blend membrane measured at 28°C

Table 5. Gas transport properties of the $2N^+$TEOS/PEBAX blend membrane measured in the dry state at 23°C. The $2N^+$ compound was titrated with HCl from pH=10.5 to pH=1.3 and then hydrolyzed in the presence of 18 mol % TEOS.

Table 6. CO_2 permeability and diffusion activation energies for $2N^+$TEOS/PEBAX membrane.

Schemes

Scheme 1. Chemical structures of the $1N^+$ and $2N^+$ compounds before the silane hydrolysis.

Scheme 2. Hydrolysed $2N^+$ compound

Scheme 3. Structure of the $2N^+$ compound obtained by the hydrolysis in the presence of TEOS in acid conditions ($2N^+$TEOS).

Figures

Figure 1. An example of humid gas permeation through the polymeric membrane.

Figure 2. TGA of the $1N^+$ and $2N^+$ compounds.

Figure 3. DSC of the $1N^+$ and $2N^+$ compounds.

Figure 4. Titration of fresh water solutions of $1N^+$ and $2N^+$ compounds and comparison to the $1N^+$ solution exposed for 4 month to the air.

Figure 5. Time-lags measured in experiments of the CO_2 diffusion through $2N^+$/PEBAX membrane. The membranes were degassed at 90°C after each measurement at temperature bellow 60°C. Dotted line is drawn according to the Arrhenius plot parameters.

Figure 6. Arrhenius plot of permeability, diffusion and solubility coefficients for CO_2 transport in $1N^+$/PEBAX blend membrane.

Figure 7. Dependence of the N_2 transport parameters on the feed pressure for $2N^+$/PEBAX membrane determined at 75°C.

*) Time-lag in s; Permeability (P) in Barrer; Diffusion coefficient (D) in 10^{-7} cm^2s^{-1}; Solubility (S) in 10^{-4} cm^3(STP) $cm^{-3}cmHg^{-1}$.

Figure 8. Dependence of the CO_2 transport parameters on the feed pressure for $2N^+$ /PEBAX membrane determined at 75°C.

*) Time-lag in s; Permeability (P) in Barrer; Diffusion coefficient (D) in 10^{-9} cm^2s^{-1}; Solubility (S) in 10^{-3} cm^3(STP) $cm^{-3}cmHg^{-1}$.

Figure 9. Arrhenius plot of the solubility coefficients in $2N^+$TEOS/PEBAX membranes

Figure 10. Arrhenius plot for hydrogen diffusion and permeability through the $2N^+$TEOS/PEBAX membrane.

Figure 11. Arrhenius plot for CO_2 diffusion and permeability trough the $2N^+$TEOS/PEBAX membrane.

Tables

Table 1. Comparison of the experimental (TGA) and calculated residue values for $1N^+$ and $2N^+$ compounds

Compound	Silane residue, (g mol^{-1})	Calculated silica content, wt%	TGA residue, wt%
$1N^+$	80	22	29
$2N^+$	80	16	20

Table 2. Gas transport properties of the $1N^+$/PEBAX blend membrane measured in the dry state at 23°C.

Gas	$D*10^8$ ($cm^2 s^{-1}$)	E_D ($kJ mol^{-1}$)	P (Barrer)	E_P ($kJ mol^{-1}$)	$S*10^3$, (cm^3(STP) $cm^{-3}cmHg^{-1}$)	ΔH_S ($kJ mol^{-1}$)
H_2	111	25.2	2.23	30.6	0.2	5.4
N_2	15.7	34.9	0.32	35.7	0.2	0.8
O_2	21.2	31.9	0.85	31.7	0.4	-0.2
CO_2	0.61	24.2	17	18.0	280	-6.2

Selectivity i/j

	D_i/D_j	P_i/P_j	S_i/S_j
CO_2/N_2	0,039	53	1370
CO_2/H_2	0,0055	7,6	1390

Table 3. Gas transport parameters of pure dry PEBAX MH 1657membrane measured at 28°C

Gas	$D*10^8$ ($cm^2 s^{-1}$)	P (Barrer)	$S*10^3$, ($cm^3(STP)cm^{-3}cmHg^{-1}$)
H_2	281	8.3	0.30
O_2	66	3.8	0.58
N_2	43	1.5	0.34
CO_2	43	82	19

Selectivity i/j

	D_i/D_j	P_i/P_j	S_i/S_j
CO_2/N_2	1	56	56
CO_2/H_2	0.15	9.9	64

Table 4. Gas transport properties of the $2N^+$/PEBAX blend membrane measured at 28°C

Gas	$D*10^8$ ($cm^2 s^{-1}$)	E_D (kJ mol^{-1})	P (Barrer)	E_P (kJ mol^{-1})	$S*10^3$, (cm^3(STP) $cm^{-3}cmHg^{-1}$)	ΔH_S (kJ mol^{-1})
H_2	230	27.9	3.7	34.6	0.16	6,7
N_2	49	34.0	0.69	37.2	0.14	3.2
O_2	41	31.9	1.6	33.2	0.38	1.3
CO_2	1.21	21.5	26	20.5	214	-1.0

Selectivity

	D_i/D_j	P_i/P_j	S_i/S_j
CO_2/N_2	0.025	38	1540
CO_2/H_2	0.005	7.1	1350

Table 5. Gas transport properties of the $2N^+$TEOS/PEBAX blend membrane measured in the dry state at 23°C. The $2N^+$ compound was titrated with HCl from pH=10.5 to pH=1.3 and then hydrolyzed in the presence of 18 mol % TEOS.

Part. 1. Membrane heating without CO_2 measurements

Gas	$D*10^8$ (cm^2s^{-1})	E_D ($kJ\ mol^{-1}$)	P (Barrer)	E_P ($kJ\ mol^{-1}$)	$S*10^3$ (cm^3(STP) $cm^{-3}cmHg^{-1}$)	ΔH_S ($kJ\ mol^{-1}$)
H_2	77.2	29.2	1.28	31.8	0.17	2.6
N_2	11.3	38.6	0.19	37.8	0.20	-0.8
O_2	17.5	34.7	0.54	32.6	0.31	-2.1

Part 2. Membrane cooling with CO_2 measurements

Gas	$D*10^8$ (cm^2s^{-1})	E_D ($kJ\ mol^{-1}$)	P (Barrer)	E_P ($kJ\ mol^{-1}$)	$S*10^3$ (cm^3(STP) $cm^{-3}cmHg^{-1}$)	ΔH_S ($kJ\ mol^{-1}$)
H_2	85.7	26.8	1.28	31.2	0.15	4.4
N_2	12.1	34.2	0.21	34.8	0.17	0.6
O_2	18.1	30.6	0.54	30.6	0.30	0
CO_2	10.6	see Table 6	11.8	see Table 6	11.2	

Selectivity i/j (cooling experiment)

	D_i/D_j	P_i/P_j	S_i/S_j
CO_2/N_2	0.87	56	66
CO_2/H_2	0,12	9,2	75

Table 6. CO_2 permeability and diffusion activation energies for $2N^{+}$TEOS/PEBAX membrane.

Curve part	E_d, (kJ/mol)	E_p, (kJ/mol)
Average	30.9	17.3
Above 60°C	27.8	15.0
Below 60°C	34.8	19.4

Schemes

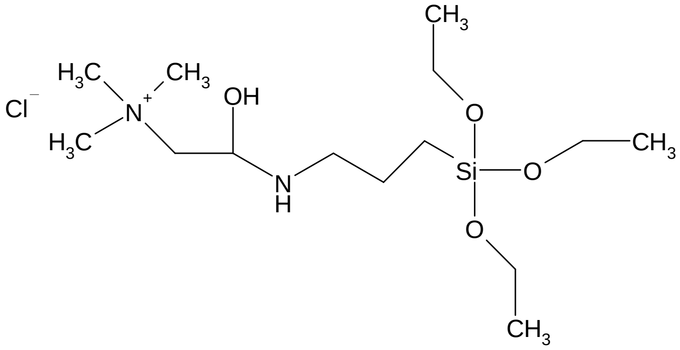

$1N^+$

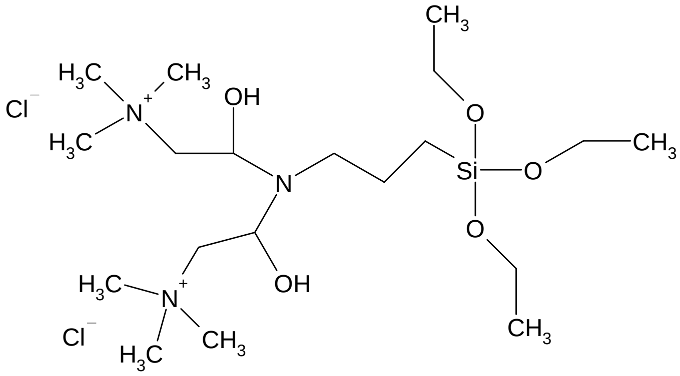

$2N^+$

Scheme 1. Chemical structures of the $1N^+$ and $2N^+$ compounds before the silane hydrolysis.

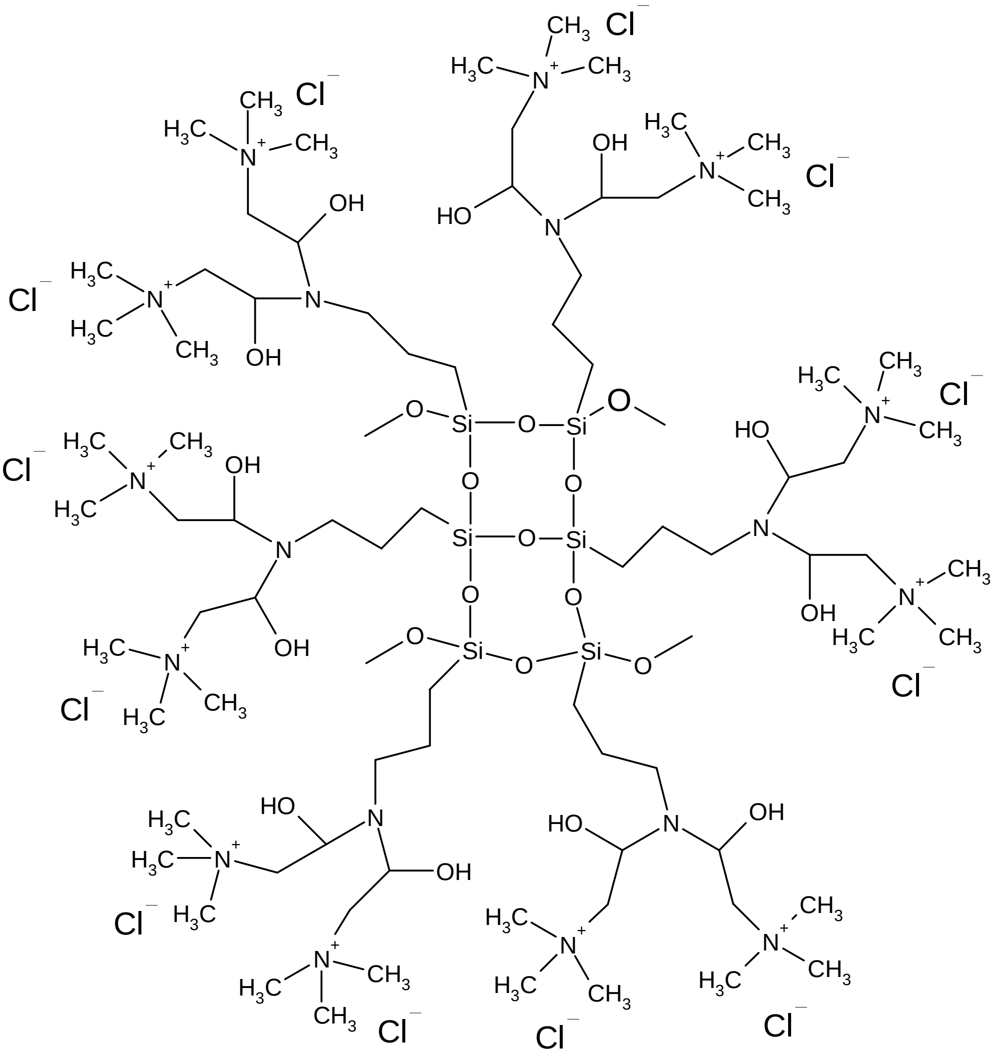

Scheme 2. Hydrolysed $2N^+$ compound

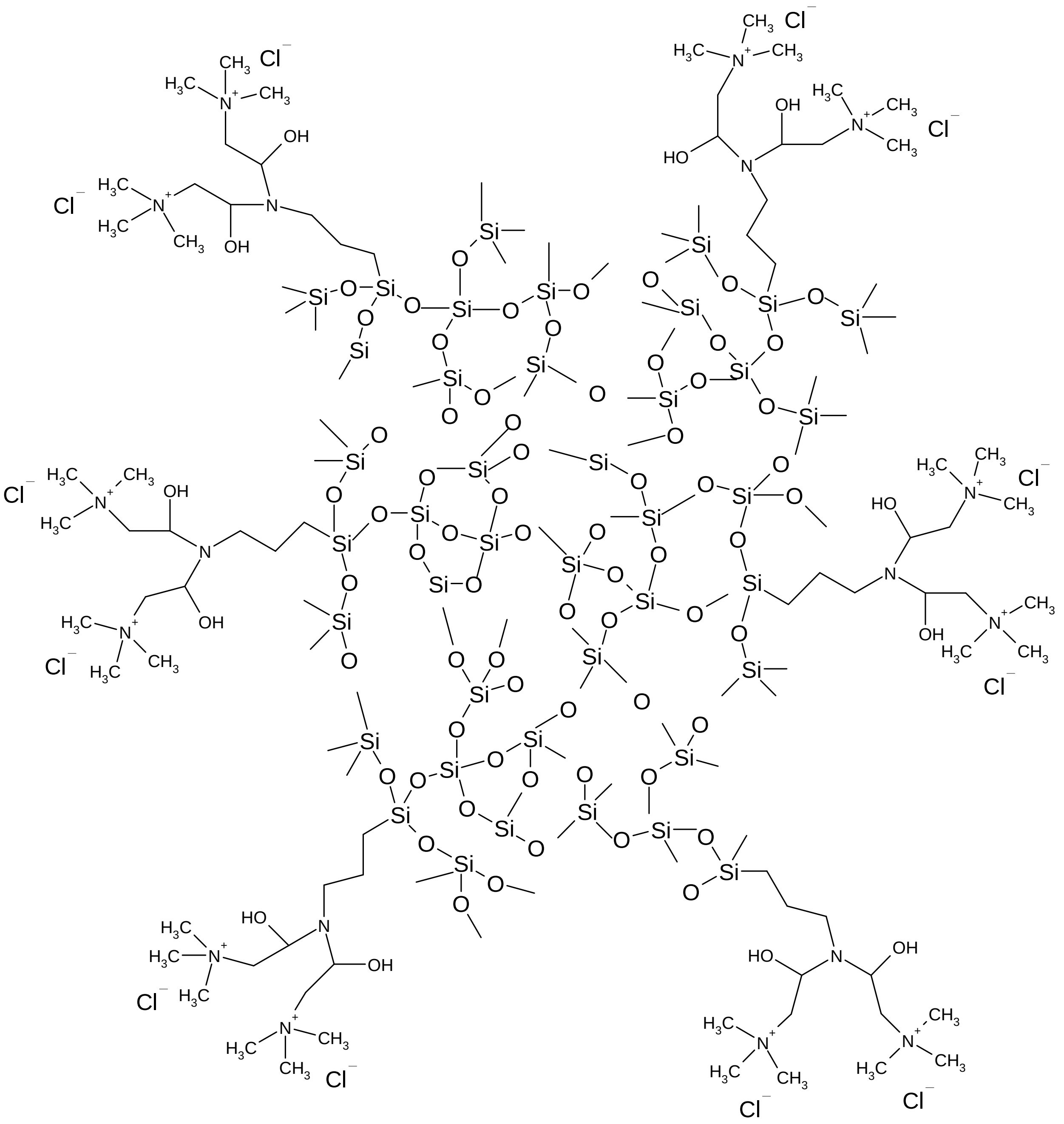

Scheme 3. Structure of the $2N^+$ compound obtained by the hydrolysis in the presence of TEOS in acid conditions ($2N^+$TEOS).

Figures

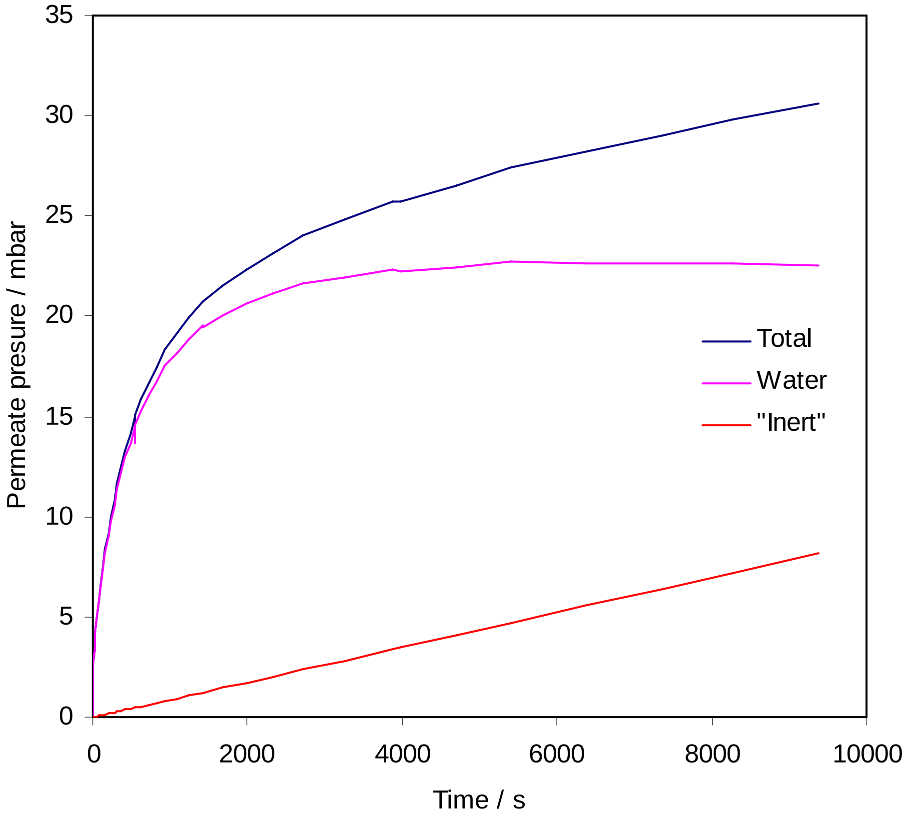

Figure 1. An example of humid gas permeation through the polymeric membrane.

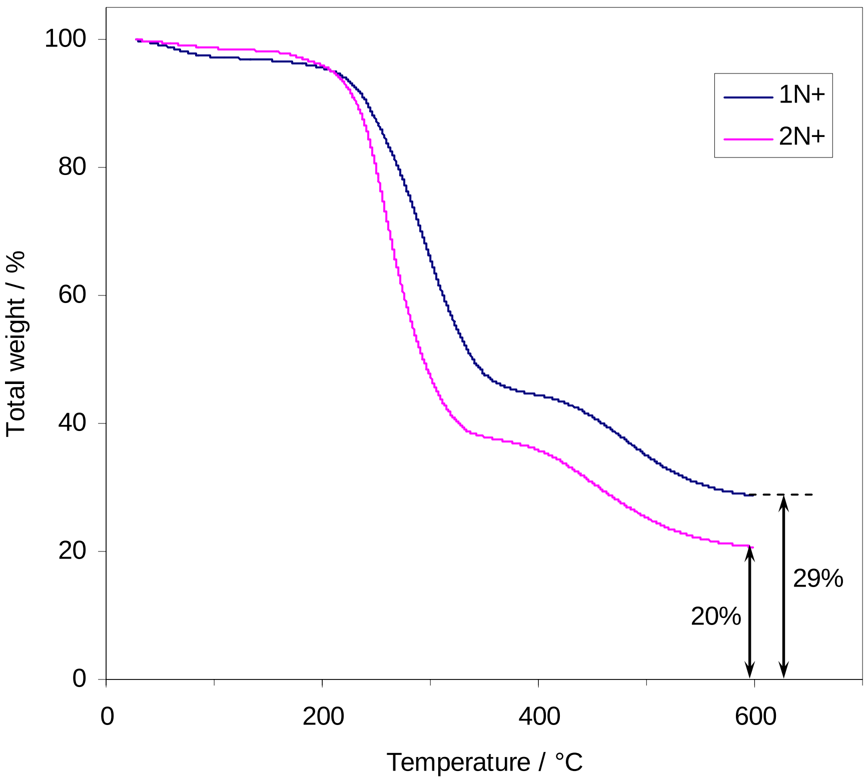

Figure 2. TGA of the $1N^+$ and $2N^+$ compounds.

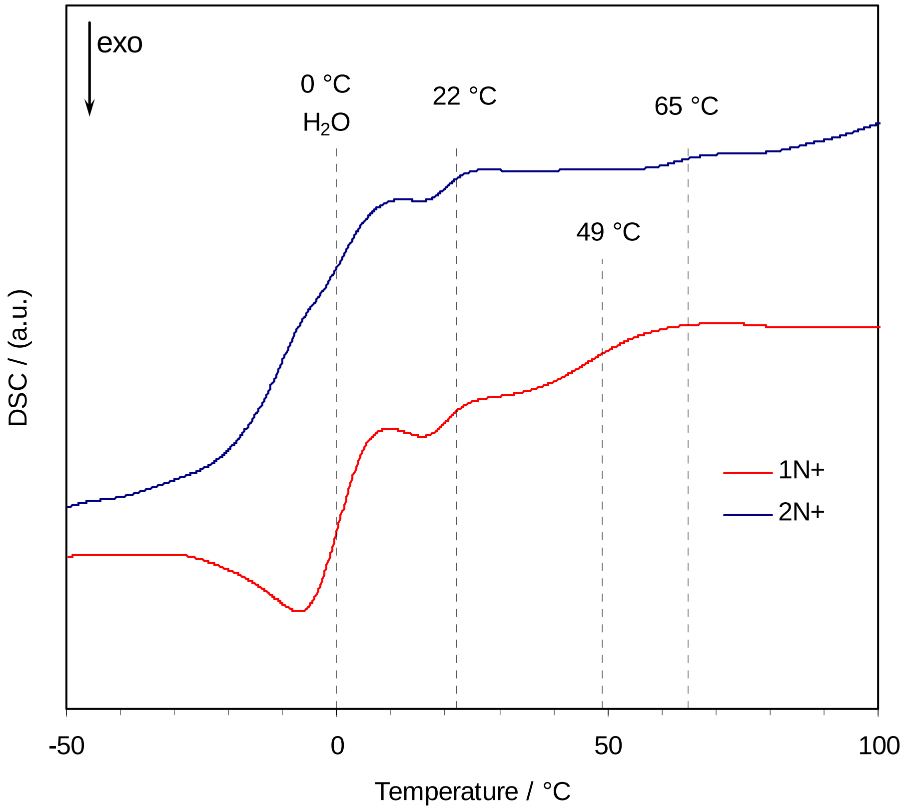

Figure 3. DSC of the $1N^+$ and $2N^+$ compounds.

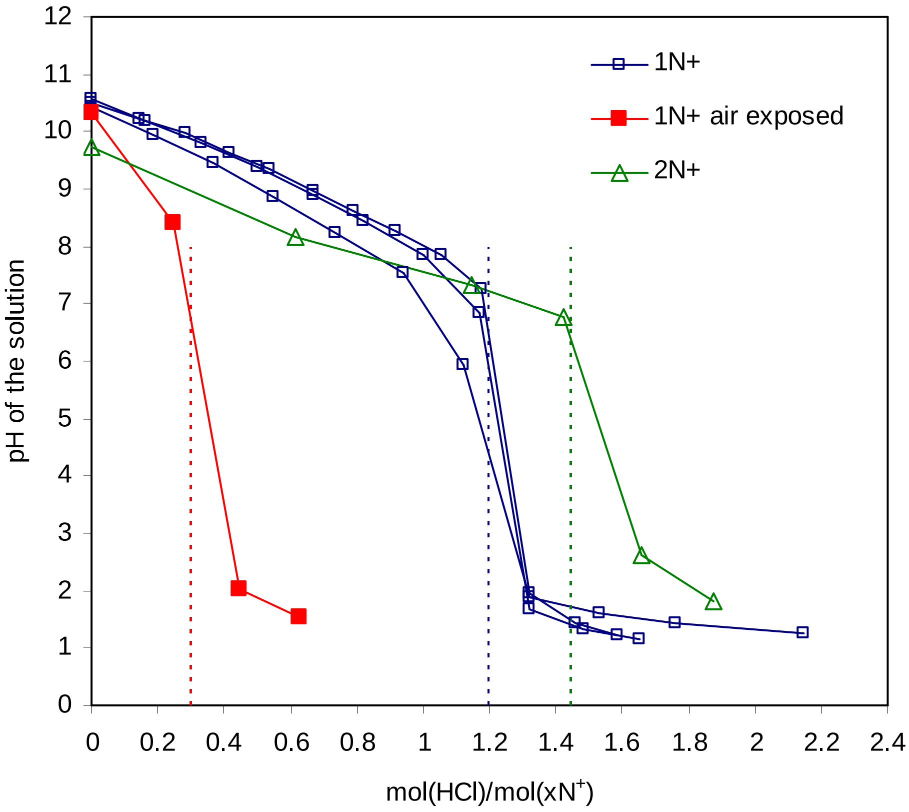

Figure 4. Titration of fresh water solutions of 1N$^+$ and 2N$^+$ compounds and comparison to the 1N$^+$ solution exposed for 4 month to the air.

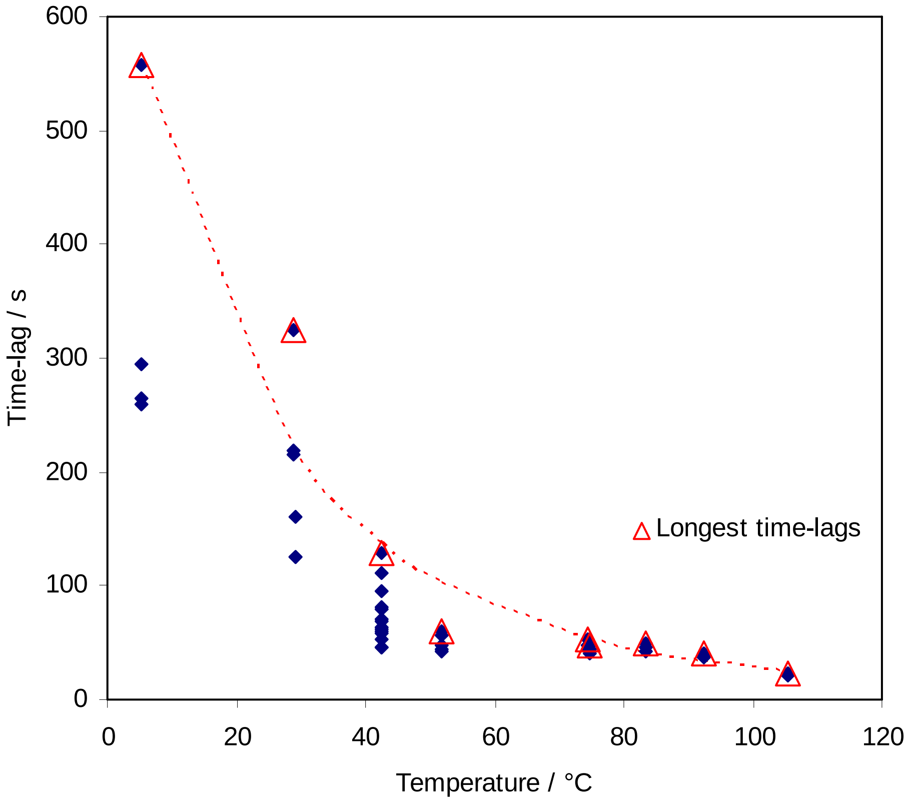

Figure 5. Time-lags measured in experiments of the CO_2 diffusion through $2N^+$/PEBAX membrane. The membranes were degassed at 90°C after each measurement at temperature bellow 60°C. Dotted line is drawn according to the Arrhenius plot parameters.

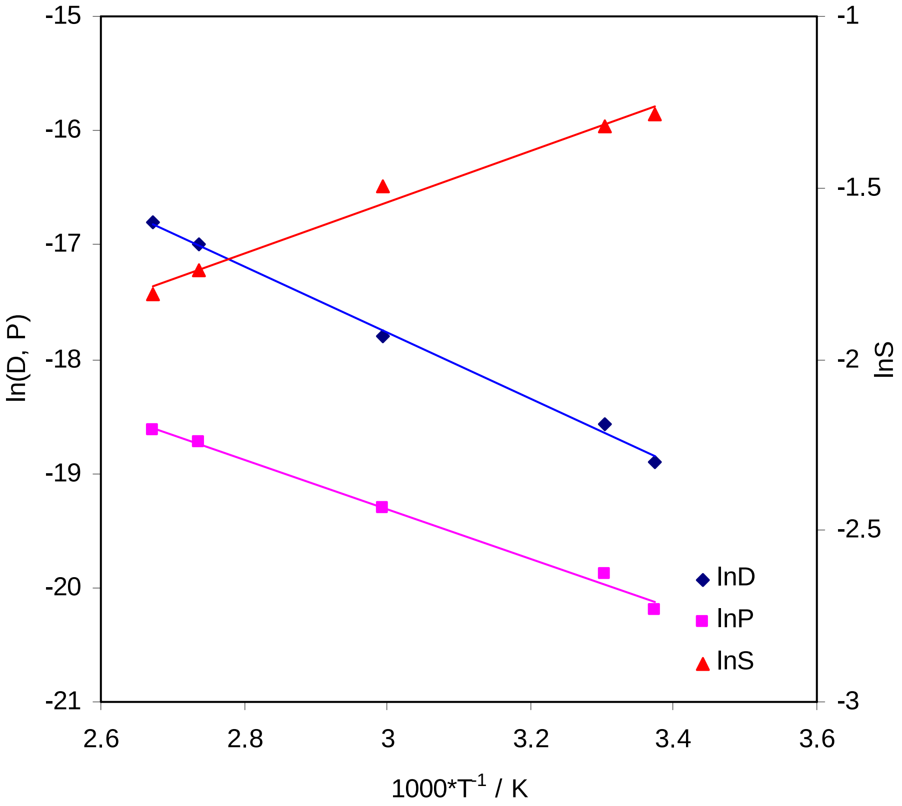

Figure 6. Arrhenius plot of permeability, diffusion and solubility coefficients for CO_2 transport in $1N^+$/PEBAX blend membrane

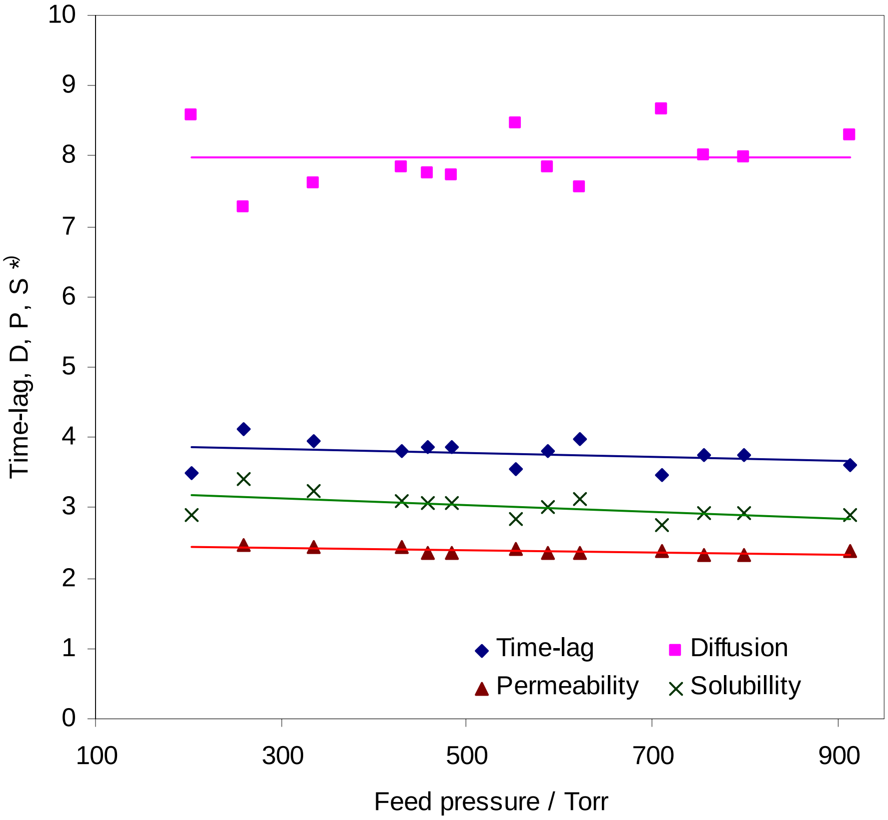

Figure 7. Dependence of the N_2 transport parameters on the feed pressure for $2N^+$/PEBAX membrane determined at 75°C.

*) Time-lag in s; Permeability (P) in Barrer; Diffusion coefficient (D) in 10^{-7} cm^2s^{-1}; Solubility (S) in 10^{-4} cm^3(STP) $cm^{-3}cmHg^{-1}$

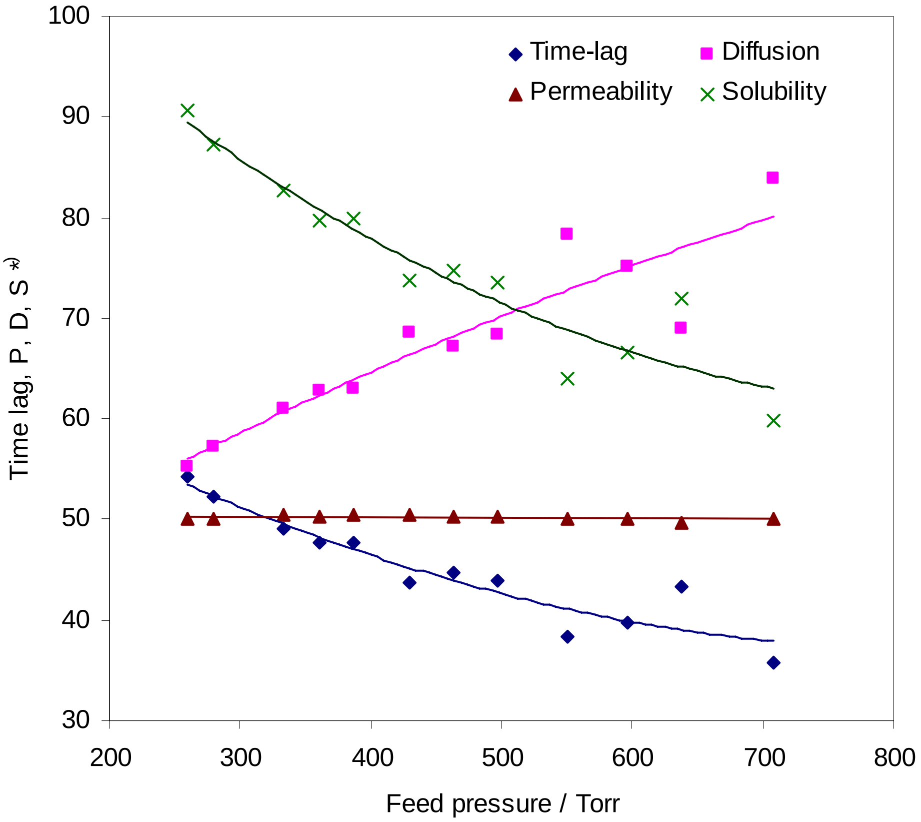

Figure 8. Dependence of the CO_2 transport parameters on the feed pressure for $2N^+$ /PEBAX membrane determined at 75°C.

*) Time-lag in s; Permeability (P) in Barrer; Diffusion coefficient (D) in 10^{-9} cm^2s^{-1}; Solubility (S) in 10^{-3} $cm^3(STP)$ $cm^{-3}cmHg^{-1}$

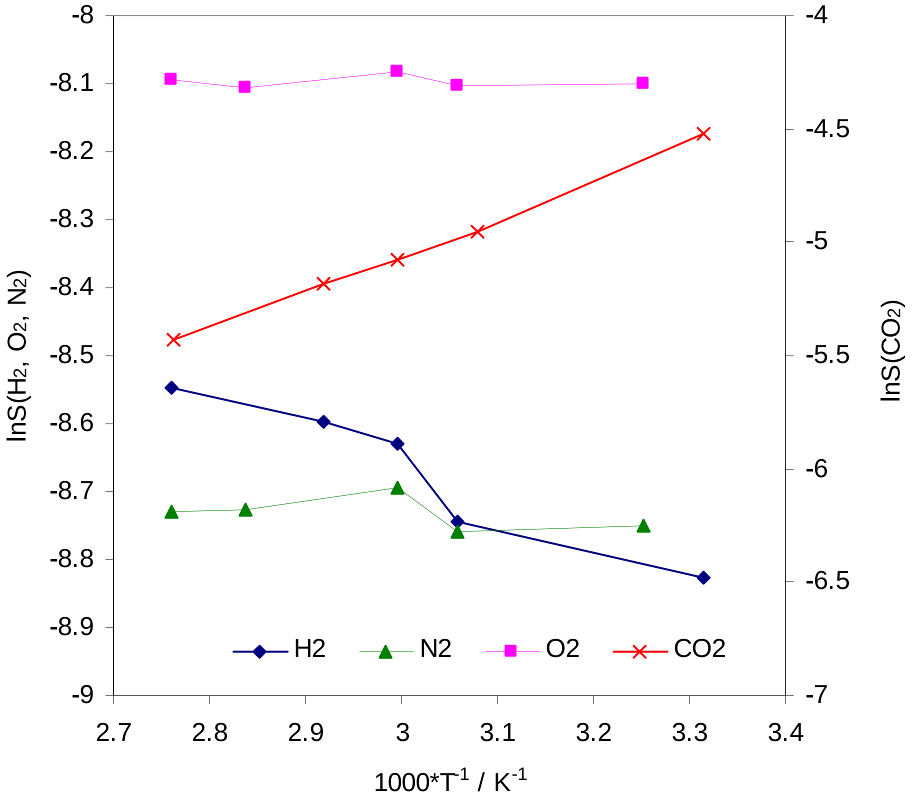

Figure 9. Arrhenius plot of the solubility coefficients in $2N^+$TEOS/PEBAX membranes

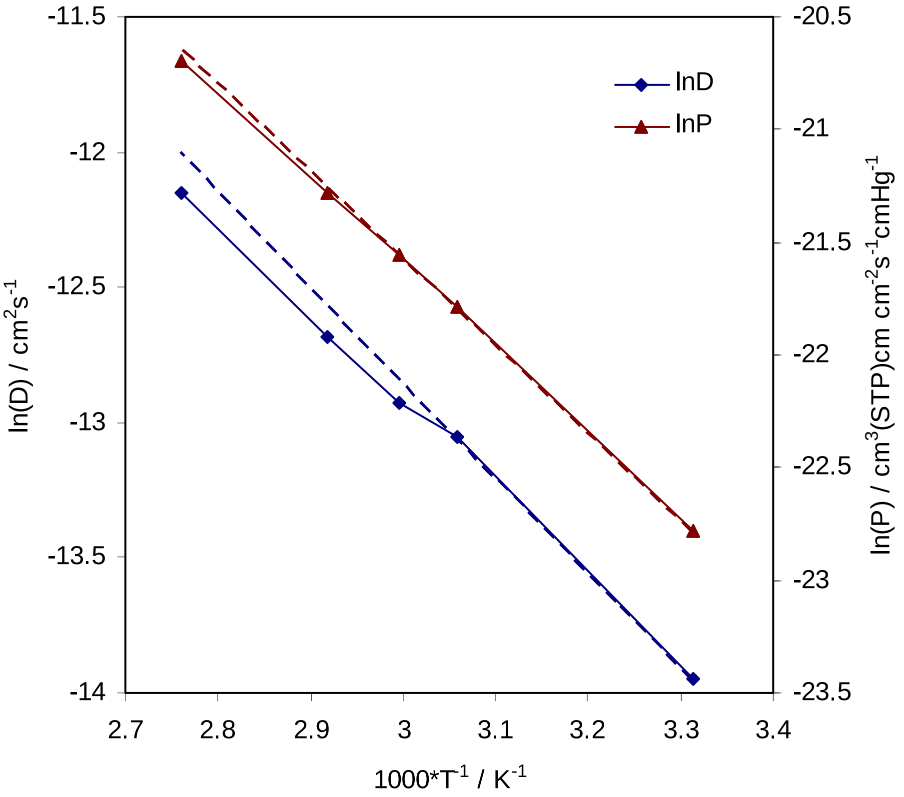

Figure 10. Arrhenius plot for hydrogen diffusion and permeability through the 2N$^+$TEOS/PEBAX membrane.

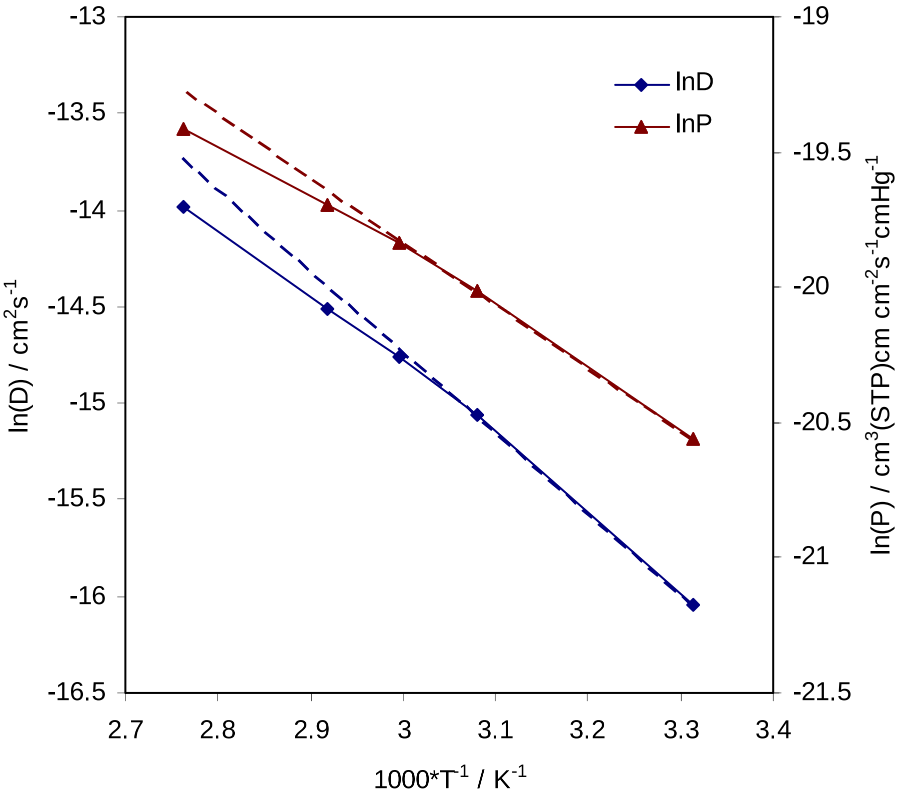

Figure 11. Arrhenius plot for CO_2 diffusion and permeability trough the $2N^+$TEOS/PEBAX membrane.